THE JOURNAL OF PHYSICAL CHEMISTRY A

 VOLUME 107, NUMBER 15, APRIL 17, 2003

ARTICLES

Predissociation of Excited Acetylene in the $\tilde{A}^1A_u$ State around the Adiabatic Dissociation Threshold as Studied by LIF and H-Atom Action Spectroscopy

Nami Yamakita,*,† Sayoko Iwamoto,† and Soji Tsuchiya‡

Department of Chemical and Biological Sciences, Faculty of Science, Japan Women's University, Mejirodai, Bunkyo-ku, Tokyo 112-8681, Japan

Received: July 31, 2002; In Final Form: December 2, 2002

The LIF and H-atom action spectra of the $\tilde{A}-\tilde{X}$ transition of acetylene in a supersonic jet were observed in the excitation-energy range of 47 000−50 600 cm^{-1}, where 60 vibrational states were identified in the $\tilde{A}$ state through rotational analyses of respective bands. Most of these states originate from anharmonic couplings of the Franck−Condon-allowed 2^m3^n states with the 4^i6^j states where $i + j =$ even. This fact is consistent with the determined rotational constants of respective states whose values are mostly between those of the 2^m3^n($m \leq 1$, $n \leq 4$) and the 4^1 or 6^1 state. The line intensities of the H-atom action spectra increase at the higher excitation energies, indicating more efficient predissociation. The lifetimes of respective excited states were evaluated from the observed spectral line widths. In a higher excitation-energy region, the lifetime is shortened from 100 ps at 47 000 cm^{-1} to 25 ps at 50 600 cm^{-1}, which exceeds the adiabatic dissociation threshold of the $\tilde{A}$ state by 933 cm^{-1} and is the wavelength limit (197 nm) of the third harmonic of the dye laser. To excite acetylene in the higher excitation energies, vibrationally excited acetylene, which was prepared by irradiation with an IR laser, was excited further by a UV laser. Utilizing this IR−UV double-resonance method, acetylene could be excited up to 53 500 cm^{-1}, which corresponds to 187 nm. Beyond 50 600 cm^{-1}, the lifetime of excited acetylene becomes longer, around 100 ps at 51 100 cm^{-1}. This sudden increase in the lifetime is attributed to the predissociation mechanism changes from the triplet state-mediated dissociation to the direct dissociation on the $\tilde{A}$ state surface. This fact is also supported by the observed average kinetic energies of H atoms estimated from the Doppler line widths of the REMPI spectral lines of H atoms; below 50 600 cm^{-1}, the kinetic energy is in proportion to the excitation energy, whereas beyond 50 600 cm^{-1}, the observed average kinetic energies are around 1000−2000 cm^{-1}, which are a little smaller than the excess energy for the production of $C_2H(\tilde{A}) + H$. It was found that the predissociation mechanism or efficiency is not dependent on the vibrational parity, gerade or ungerade, of the initial excited state. This is attributed to the anharmonic coupling between the ν_3' and ν_4'/ν_6' vibrational modes.

Introduction

The photodissociation mechanism of acetylene (C_2H_2) into $C_2H + H$ in the ultraviolet or vacuum ultraviolet region has been investigated extensively in recent years. The dissociation energy D_0(HCC−H) of acetylene in the $\tilde{X}$ state was determined first by Wodtke and Lee[1] to be 46 190 ± 700 cm^{-1} on the basis of the observed kinetic energy of the C_2H fragment. Since then, several groups[2−12] have reported slightly different values, of which Mordaunt and Ashfold[12] obtained the most precise value, 46 074 ± 8 cm^{-1}. The electronically excited state $\tilde{A}\ ^1A_u$ of acetylene is adiabatically correlated with $C_2H(\tilde{A}^2\Pi) + H$ in the

* To whom correspondence should be addressed. E-mail: yamakita@fc.jwu.ac.jp.
† Japan Women's University.
‡ Present address: Department of Chemistry, Faculty of Science, Josai University, Sakado, Saitama 350-0295, Japan.

10.1021/jp0217785 CCC: $25.00
Published on Web 03/20/2003

TABLE 1: Normal Modes of Acetylene in the $\tilde{A}\ ^1A_u$ State

mode	normal coordinate	fundamental frequency/cm^{-1}	vibrational symmetry
ν_1'	sym. CH str.	2880[a]	a_g
ν_2'	CC str.	1387[b]	a_g
ν_3'	trans bend	1048 [b]	a_g
ν_4'	torsion	765[c]	a_u
ν_5'	antisym. CH str.	2857[d]	b_u
ν_6'	cis bend	768[c]	b_u

[a] Reference 53. [b] Reference 51. [c] Reference 46. [d] Reference 47.

planar geometry, and the $\tilde{A}$ state of C_2H is located 3693 cm^{-1} from the ground vibrational level of the $\tilde{X}$ state.[13,14] Thus, the photolysis at 193.3 nm whose photon energy exceeds 46 074 + 3693 = 49 767 cm^{-1} is likely to produce C_2H in the $\tilde{A}$ state. In fact, C_2H in the $\tilde{A}$ as well as $\tilde{X}$ states was found in the photodissociation products at 193.3 nm by Balko et al.[10]

The predissociation of acetylene in the $\tilde{A}$ rovibronic states was evidenced first by Fujii et al.,[15,16] who found a sudden decrease in the fluorescence quantum yield in the 3^4 vibronic state (refer to Table 1 for the definition of the vibrational modes), whose energy corresponds to the dissociation energy. Later, Suzuki and co-workers[17,18] and Mordaunt et al.[19] confirmed the predissociation directly by the detection of the produced H atoms and suggested a predissociation process over an exit barrier with a height of 560 cm^{-1} [17,18] or 540 cm^{-1} [19] on the basis of kinetic energy measurements. Furthermore, Suzuki's group found a slow predissociation rate[18] as well as a very small fluorescence quantum yield[20] of acetylene in a rovibronic level of the $\tilde{A}$ state around the dissociation threshold and proposed a mechanism in which intersystem crossing to a triplet state occurs prior to the dissociation. The singlet−triplet interaction of acetylene in the $\tilde{A}$ state had already been proven by several spectroscopic methods such as the Zeeman quantum beat,[21−23] Zeeman anticrossing,[24−26] sensitized phosphorescence (SP),[27,28] and laser-excited metastable (LEM) spectroscopy.[29,30] The singlet−triplet coupling and the predissociation mechanism were also discussed by means of ab initio MO calculations.[31−37] Of these, Cui et al.[36,37] proposed a predissociation scheme through three triplet states, T_3, T_2, and T_1. This mechanism was supported by Mordaunt et al.'s finding[19] that the product $C_2H(\tilde{X})$ is mostly excited in the bending mode and that its rotational distribution is bimodal, indicating two competing mechanisms including the $S_1-T_3-T_2-T_1$ and S_1-T_1 transitions prior to the dissociation.

As already mentioned, the photodissociation at 193.3 nm yields the product C_2H in the $\tilde{X}$ state as well as in the $\tilde{A}$ state.[1,10−12] However, Zhang et al.[38] reported that if acetylene prepared in the $\nu_1'' + 3\nu_3''$ state is photodissociated at 248 nm then the product C_2H is mostly in the $\tilde{A}$ state. In this case, the photolysis energy is higher than the 193.3 nm photon energy by 1200 cm^{-1}. They also found that the photolysis at 121.6 nm yields C_2H in the $\tilde{A}$ state exclusively. This result, which was interpreted by Cui et al.'s ab initio calculation,[36] was attributed to the fact that the 193.3 nm photon energy is insufficient to surmount the transition state on the S_1 adiabatic surface, whereas the vibrational energy of acetylene is used efficiently for dissociation through the adiabatic path. The IR−UV photolysis was also reported by Rosenwaks and co-workers,[39−42] who found some enhancement of the CH bond dissociation by the vibrational excitation of acetylene in the $2\nu_1'' + 3\nu_3''$ state. The photodissociation at 193.3 nm was discussed in terms of the state analysis of the product C_2H by Fletcher and Leone[43] and by Hsu et al.[44] Both experiments indicate that the product C_2H is distributed mostly in highly excited bending states of the $\tilde{X}$ state.

TABLE 2: Vibrational Term Values and Rotational Constants $T_0 + A$, B, and C Determined by the Least-Squares Fitting of the Observed Rotational Lines in the Respective Numbered Bands in Figure 2a

band no.	$T_0 + A$/cm^{-1}	B/cm^{-1}	C/cm^{-1}	std dev
1	47 148.01(1)	1.124(2)	1.026(2)	0.032
2	47 207.32(2)	1.129(2)	1.021(2)	0.057
3	47 261.01(2)	1.121(2)	1.012(2)	0.049
4[a]	*47 328.47(6)*	*1.192(15)*	*0.876(15)*	*0.145*
5	47 390.00(2)	1.102(2)	1.010(2)	0.048
6	47 512.47(1)	1.111(2)	1.012(2)	0.030
7	47 678.62(2)	1.121(3)	1.018(3)	0.051
8	48 028.66(1)	1.118(2)	1.020(2)	0.036
9	48 052.40(2)	1.106(2)	1.002(2)	0.057
10	48 070.67(1)	1.126(2)	1.037(2)	0.043
11	48 125.97(1)	1.113(2)	1.032(1)	0.046
12	48 133.04(1)	1.086(1)	1.066(1)	0.021
13	48 161.14(1)	1.126(1)	1.039(1)	0.013
14	48 231.80(1)	1.080(1)	1.058(1)	0.023
15	48 236.26(2)	1.121(2)	1.034(2)	0.042
16[a]	*48 257.65(1)*	*1.159(2)*	*1.025(2)*	*0.043*
17	48 278.35(2)	1.116(2)	1.026(2)	0.049
18	48 406.60(2)	1.117(2)	1.002(2)	0.054
19	48 532.92(2)	1.111(2)	1.010(2)	0.047
20	48 578.37(1)	1.109(2)	1.103(2)	0.024
21	48 580.08(1)	1.112(3)	1.077(3)	0.031
22	48 611.08(2)	1.123(2)	1.032(2)	0.046
23	48 638.28(1)	1.138(2)	1.007(2)	0.041
24	48 671.14(2)	1.110(2)	1.065(2)	0.045
25[a]	*48 716.17(2)*	*1.003(5)*	*1.061(5)*	*0.201*
26[a]	*48 783.90(2)*	*1.055(4)*	*1.047(4)*	*0.050*
27	48 877.32(1)	1.110(2)	1.054(2)	0.035
28	48 981.35(1)	1.097(5)	1.024(5)	0.050
29	49 041.82(1)	1.108(2)	1.012(2)	0.050
30	49 094.17(1)	1.116(2)	1.009(2)	0.028
31	49 106.10(1)	1.117(2)	1.038(2)	0.038
32	49 157.25(1)	1.133(2)	1.047(2)	0.033
33	49 183.52(1)	1.085(2)	1.019(2)	0.029
34	49 186.66(1)	1.099(2)	1.029(2)	0.027
35	49 282.54(2)	1.099(5)	1.054(5)	0.053
36	49 283.55(1)	1.111(2)	1.041(2)	0.038
37	49 429.60(1)	1.112(5)	1.031(5)	0.045
38[a]	*49 496.33(1)*	*1.128(3)*	*1.048(3)*	*0.049*
39[a]	*49 502.19(1)*	*1.085(2)*	*1.044(2)*	*0.050*
40[a]	*49 523.69(2)*	*1.194(5)*	*1.002(5)*	*0.060*
41[a]	*49 532.58(1)*	*1.088(3)*	*1.068(3)*	*0.031*
42	49 550.60(1)	1.105(2)	1.019(2)	0.034
43	49 589.71(1)	1.110(2)	1.061(2)	0.040
44	49 601.96(2)	1.149(2)	1.032(2)	0.057
45	49 662.95(1)	1.124(2)	1.060(2)	0.036
46	49 799.33(1)	1.115(2)	1.096(2)	0.042
47	49 892.73(2)	1.107(2)	1.036(2)	0.052
48	49 982.95(1)	1.128(2)	1.019(2)	0.030
49	50 003.49(2)	1.126(2)	1.048(2)	0.056
50	50 005.93(1)	1.125(2)	1.004(2)	0.046
51[a]	*50 035.09(2)*	*1.074(2)*	*1.041(2)*	*0.054*
52[a]	*50 038.21(2)*	*1.069(2)*	*1.068(2)*	*0.050*
53[a]	*50 054.52(3)*	*1.134(5)*	*1.024(5)*	*0.096*
54[a]	*50 086.31(1)*	*1.043(2)*	*1.028(2)*	*0.038*
55	50 189.78(2)	1.097(2)	1.035(2)	0.051
56	50 421.19(1)	1.128(2)	1.015(2)	0.045
57	50 424.20(1)	1.127(2)	1.050(2)	0.040
58[a]	*50 461.10(1)*	*1.144(2)*	*0.991(2)*	*0.039*
59[a]	*50 462.37(2)*	*1.085(2)*	*1.017(2)*	*0.053*
60	50 504.08(1)	1.110(2)	1.057(2)	0.050

[a] The italic data should be assumed to be tentative since in these bands the number of assigned rotational transitions is less than 10.

In the previous experiments on the photolysis around the adiabatic dissociation threshold in the $\tilde{A}$ state, the photolysis energy is limited to a fixed value such as that of 193.3 nm. Furthermore, in this energy region, the only available spectral data of the $\tilde{A}-\tilde{X}$ transition is that reported by Van Craen et al.,[45] which covers 205−193 nm and is composed of a congested

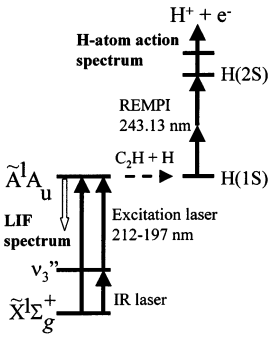

Figure 1. Excitation and detection scheme in the present experiment.

continuumlike spectrum. Our motivation in this work is to clarify the rovibronic level structure of highly excited acetylene in the Ã state using supersonic jet spectroscopy and furthermore to observe the dissociation efficiencies that are specific to the excited states. For this research object, laser-induced fluorescence (LIF) and H-atom action spectroscopy have been applied to elucidate the photodissociation of acetylene in the excited rovibronic levels below and above the adiabatic dissociation threshold in the Ã state in the region from 212 to 197 nm.

In the single-photon Ã−X̃ transition of acetylene, the vibrational states in the upper and lower electronic states must have the same symmetry with respect to the inversion symmetry operation. Thus, acetylene in the ground vibrational state of the X̃ state can be excited only to the Ã vibrational state with gerade symmetry. To excite acetylene to an ungerade vibrational state, it is necessary that acetylene be prepared in an ungerade vibrational state in the X̃ state prior to the electronic excitation. This can be achieved by the IR−UV double-resonance excitation method, and the first spectroscopic work was done by Crim and co-workers,[46−48] who could observe transitions to ungerade vibrational states 4^1, 6^1, 5^1, and 3^15^1. Their significant finding was that of strong Coriolis coupling between the 4^1 and 6^1 states, and this finding was extended to the normal mode analyses of the excited vibrational states of both gerade and ungerade symmetries.[48] Later, we confirmed the Coriolis couplings between 3^n4^1 and 3^n6^1 ($n = 2, 3$).[49] In this work, we have applied the UV single-photon and the IR−UV double-resonance excitation of acetylene in the region around the adiabatic dissociation threshold in the Ã state to observe the dissociation efficiencies from the gerade as well as ungerade vibrational states.

Experimental Section

Figure 1 shows a schematic diagram of the excitation and detection scheme in our experiment. For the UV single-photon excitation to the Ã state, acetylene in a supersonic jet in the ground state X̃ was irradiated with the excitation UV laser, the frequency-doubled or frequency-tripled output of a dye laser (Lambda Physik, Scanmate 2EX) pumped by a XeCl excimer laser (Lambda Physik, Compex 201). To generate the third harmonic of the dye laser in a wavelength region shorter than 206 nm, the frequency-doubled output was mixed with the fundamental in a BBO crystal (Inrad, Autotracker III). The energy region of the excited state covered by the present experiment was from 47 000 to 50 600 cm^{-1} (212−197 nm). The resolution of the UV laser was 0.5 cm^{-1} with a grating cavity and 0.075 cm^{-1} with an etalon-inserted cavity, which was confirmed by the use of a wavelength meter (Burleigh WA-4500). The line width of the third harmonic of the dye laser can be assumed to be $^3/_2$ the width of the second harmonic UV laser. The excitation laser beam was not focused in order to avoid the secondary photodissociation of the primary product (ethynyl radical, $C_2H + h\nu \rightarrow C_2 + H$), and its pulse energy was on the order of 100 μJ, which was of the threshold magnitude for the REMPI detection of the produced H atoms. The jet was produced by expanding acetylene gas (Takachiho Chem. Co.) into vacuum through a pulsed nozzle with an orifice diameter of 0.8 mm and a stagnation pressure of about 0.8 atm. The laser light irradiated the jet at about 20 and 50 mm downstream from the nozzle orifice for measurements of the LIF and the H-atom action spectra, respectively. Fluorescence from excited acetylene emitted in the direction perpendicular to both the UV laser beam and the jet axis was collected by a lens system and detected by a photomultiplier (Hamamatsu, R928). To obtain the laser-induced fluorescence (LIF) spectrum, the fluorescence signal was led to an amplifier (NF, BX-31A), and its output was treated by a boxcar integrator (Stanford Research Systems, SR250) by scanning the UV laser wavelength, which was calibrated by simultaneous measurements of the optogalvanic spectrum of Ne from the hollow-cathode lamp (Hamamatsu, L2783-26KNE-FE) using the fundamental laser light. The laser power was monitored using a solar-blind photomultiplier (Hamamatsu, R166) and was recorded simultaneously to normalize the signal intensity.

The H atoms produced from excited acetylene were detected by the 2 + 1 resonantly enhanced multiphoton ionization (REMPI) method using another UV laser (243.13 nm); the frequency-doubled output of a dye laser (Lambda Physik, Scanmate 2EY) pumped by the third harmonic of the Nd:YAG laser (Continuum, Surelite III-10) irradiated the supersonic jet of acetylene from the reverse direction of the UV excitation laser after a 10 ns delay. The produced ions were collected by a repeller electrode and led through three pairs of ion lenses into a channeltron whose signal was also treated by a boxcar averager and transferred to a personal computer. The H-atom action spectrum was obtained by scanning the excitation UV laser wavelength while detecting the H atoms by the REMPI method. For measurements of the Doppler line profile, the excitation laser wavelength was fixed to a selected peak of the Ã−X̃ transition, and the ionization laser wavelength was scanned around the 243.13-nm region.

For the IR−UV double-resonance excitation, the experimental setup was described previously.[49] Acetylene in a supersonic jet was excited first to a single rotational level of the antisymmetric C−H stretching ν_3'' state[50] by irradiation with an IR laser prior to the UV excitation. The IR laser was a single-mode optical parametric oscillator, OPO (Continuum, Mirage3000), that was pumped by a frequency-doubled injection-seeded Nd:YAG laser (Continuum, Powerlite8000). After a 5 ns delay from the IR laser pulse, the UV excitation laser irradiated the jet, whose beam direction was merged with that of the IR laser by use of a UV reflector that transmitted the IR laser. The LIF and H-atom action spectroscopic methods were the same as those described for the UV single-photon excitation. By combining the IR and UV lasers, we excited acetylene in the energy region up to 53 500 cm^{-1}, which corresponds to 187 nm.

Results and Discussion

LIF Spectrum. The observed LIF spectrum in the excitation-energy region of 47 000−50 600 cm^{-1} (212.8−197.6 nm) is shown in Figure 2a. In our observed region, 60 vibrational transition bands could be identified, as indicated by the numbers attached to the respective bands. These bands are composed of a rotational line structure that is similar to that shown in Figure 3. There remain many unidentified weak spectral lines that may not be assigned as rotational transitions probably because of line overlapping or interference by signal noise.

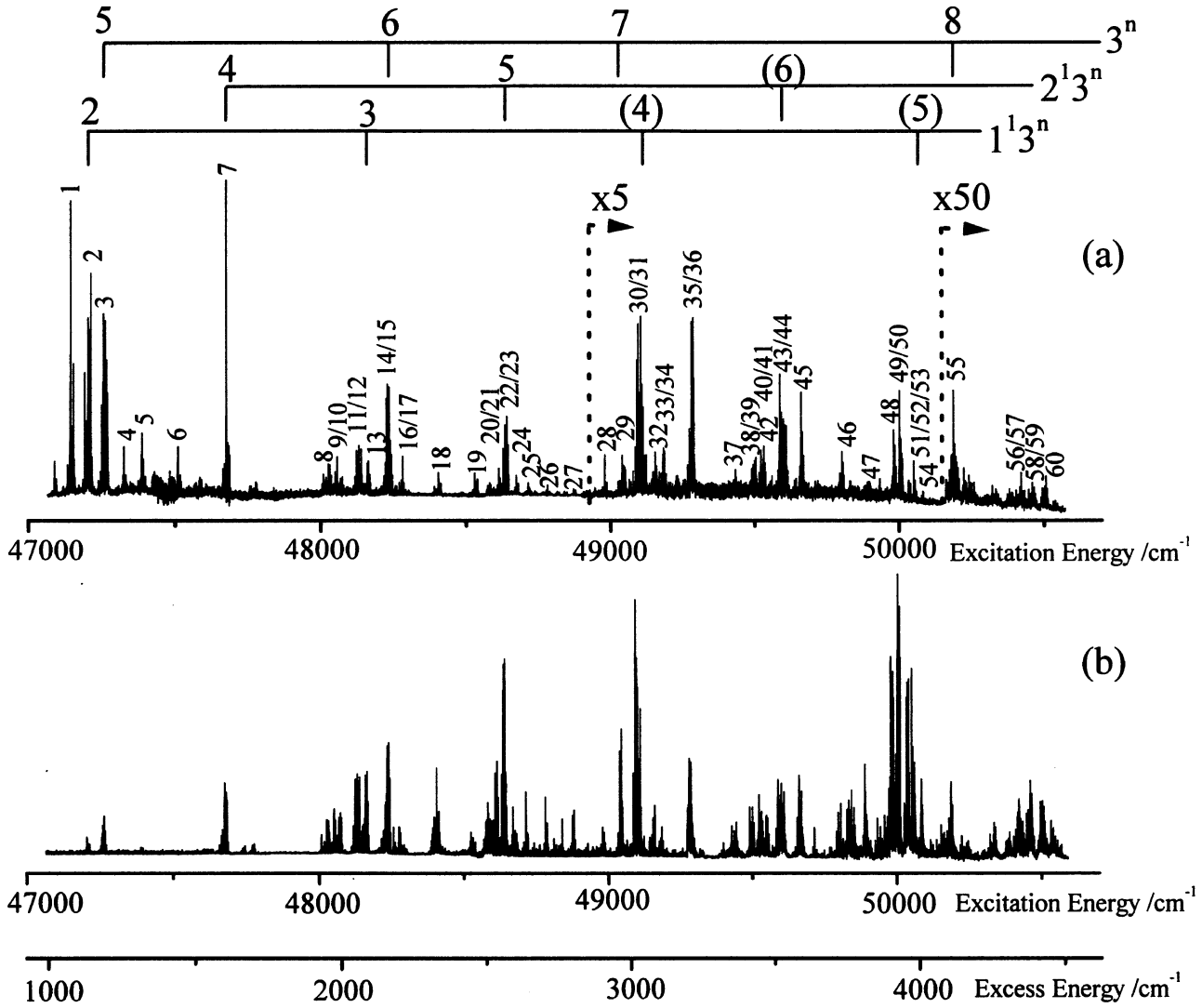

Figure 2. (a) LIF and (b) H-atom action spectra as a function of the excitation energy as well as the excess energy that is defined as the excitation energy minus the dissociation threshold of 46 074 cm^{-1}. The LIF line intensities in the higher excitation-energy region are magnified as indicated. Numbered vibrational bands are rotationally analyzed as listed in Table 2.

Acetylene in the $\tilde{A}$ state takes a trans bent structure with a C−C bond length longer than that in the $\tilde{X}$ state so that the Franck−Condon active vibrational modes of the $\tilde{A}-\tilde{X}$ transition are the trans bending ν_3' and the C−C stretching ν_2'. Thus, the band progressions of the ν_3' and ν_2' modes are likely to be the major spectral bands in the $\tilde{A}-\tilde{X}$ transition, as pointed out by Watson and co-workers.[45,51,52] They analyzed the absorption spectrum in a wide energy range and assigned the band systems to the vibrational transitions to the 3^n ($n = 0-8$), $2^1 3^n$($n = 0-5$), and $1^1 3^n$ ($n = 2, 3$) vibrational states in the $\tilde{A}$ state mostly with $K_a = 1$. In the top of Figure 2a, the tie lines mark their assigned band positions of the progressions. According to their assignments, the no. 2 band corresponds to the transition to the $1^1 3^2$ state. However, our recent new data[53] indicates that the no. 1 band must be the transition to the $1^1 3^2$ state since the transition band to the $1^1 3^1$ state is located at 46 114 cm^{-1} and the level spacing is appropriate for the no. 1 band to be the transition to the $1^1 3^2$ state. Then, it becomes uncertain whether the no. 2 band could be a member of the ν_2' and ν_3' progressions. One possible explanation is that the upper state of this band is formed by an interaction between one of the vibrational states of the aforementioned progressions and a vibrational state having no Franck−Condon factor with the ground vibrational state of the $\tilde{X}$ state. The latter state is named as a dark state, whereas the

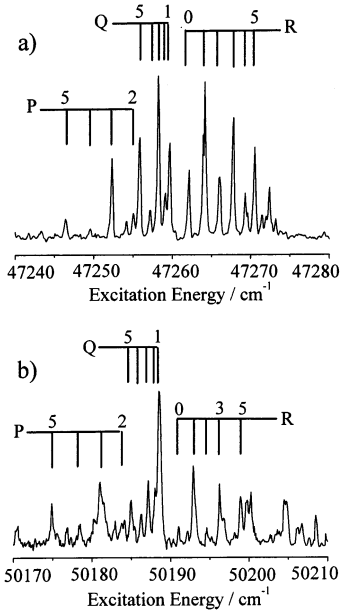

Figure 3. Examples of the rotational line structure of the LIF bands at low and high excitation energies. (a) Band 3 and (b) band 55 in Figure 2a and Table 2.

former is named as a bright state. A dark state appears through coupling with a bright state. This fact was reported for the first time in the $\tilde{A}$ state of acetylene by Scherer et al.,[54] who found a state that couples with the 3^3 state. This experimental finding was reconfirmed later by the high-resolution measurement of Drabbels et al.[55]

Regarding the ungerade vibrational states of acetylene in the $\tilde{A}$ state, the first observation of the transitions to the 4^1 and 6^1 states from the $3\nu_3''$ state of the $\tilde{X}$ state was made by Utz et al.[46] through NIR−UV double-resonance spectroscopy. Referring to Table 1, the vibrational symmetries of ν_6' and ν_4' are b_u and a_u, respectively, so that only the transition to the ν_6' state is allowed. However, they found that the two states couple strongly with each other via the Coriolis interaction to form the two mixed states to which the spectral transitions are allowed. According to their spectral analyses, the vibrational frequencies of ν_4' and ν_6' are very close to 764.9 and 768.3 cm^{-1}, respectively, and thus these two modes may play an important role in the vibrational resonance of the $\tilde{A}$ state; for instance, the perturber of the 3^3 state could be $\{b^4\}$, where $\{b^4\}$ stands for the 4^4, 4^26^2, and 6^4 states. This type of anharmonic resonance was well established in the $\tilde{X}$ state of acetylene,[56−65] where the vibrational level structure could be described as a polyad structure characterized by polyad quantum numbers n_r, n_s, and n_l,[66] which describe the vibrational resonance of the stretch−bending and stretching vibrations and that along the axial angular momentum.

Referring to Figure 2a, it is seen that the number of observed bands that may not be assigned to the ν_2' and ν_3' progressions increases in the energy region higher than 48 000 cm^{-1} and at the same time the band intensities become very small. The appearance of these bands may be attributed to the anharmonic resonance described in the previous paragraph. If an anharmonic coupling occurs between a single quantum of ν_3' and two quanta of ν_4' or ν_6', then the 3^n state splits into $(n + 1)(n + 2)/2$ states; for example, the 3^6 state yields 28 coupled states that are 3^6, $3^5\{b^2\}$, $3^4\{b^4\}$, $3^3\{b^6\}$, $3^2\{b^8\}$, $3^1\{b^{10}\}$, and $\{b^{12}\}$. In our previous dispersed fluorescence (DF) measurements[67] from two levels near the 3^6 state, it was found that the observed DF from one level consists mainly of the ν_4'' (trans bending mode) progressions, whereas that from the other level consists of the ν_5'' (cis bending mode). This was attributed to the two excited states having different vibrational characteristics; the state that yields the ν_4'' progressions is composed mostly of the ν_3' mode, whereas the other is a state coupled with the ν_4' and/or ν_6' mode.

The $\tilde{A}-\tilde{X}$ transition of acetylene is of the c type, and the rotational selection rule is $\Delta J = 0, \pm 1$ and $\Delta K_a = K_a' - l'' = \pm 1$. Since $l'' = 0$ in the ground state, $K_a = 1$ in the $\tilde{A}$ state. The rotational line structure of the respective bands, two examples of which are given in Figure 3, is simple to analyze since the maximum J is around 6 because of a low rotational temperature of 30 K. The observed rotational transitions are fitted by a rigid-rotor approximation within the residuals less than 0.05 cm^{-1}. In this calculation, the rotational constant A is assumed to be the one extrapolated from the values reported by Watson et al.,[51,52] and the constants $T_0 + A$, B, and C can be determined by the least-squares fitting of the observed transitions. In this case, the values of B and C are not sensitive to the assumed value of A. The determined constants for the identified bands in Figure 2a are listed in Table 2. In Figure 4, the determined rotational constants of B together with those reported by Watson and co-workers[51,52] are plotted as a function of the excitation energy. The B constants reported by Watson and co-workers for the 3^n ($n = 0-6$) and 2^13^n ($n = 1-4$) states are

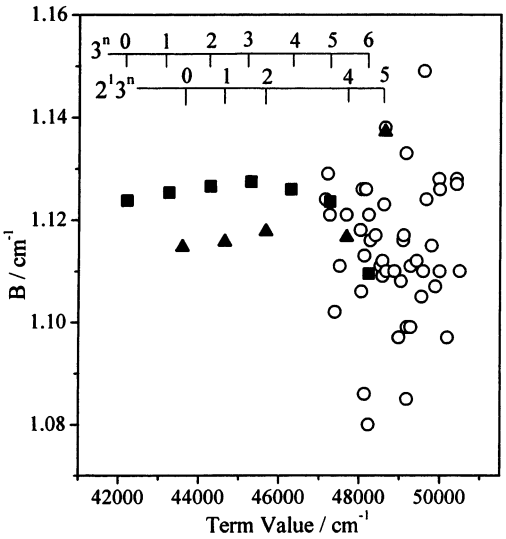

Figure 4. Determined rotational constants (○) of the upper vibrational states in the numbered bands given in Figure 2a and Table 2 along with the reported values by Watson and co-workers[51,52] for the 3^n states (■) and the 2^13^n states (▲), respectively. The tentative values given in italics in Table 2 are not plotted.

almost constant. However, above 47 000 cm^{-1}, most of the determined B values are smaller than those of Watson and co-workers and take scattered values. If the relevant state involves some contribution from the ν_b' vibration due to the anharmonic resonance, then the B constant may be closer to those of the b^n state. The B value of the 3^n ($n = 0-5$) state is around 1.125 cm^{-1}, whereas those of the 4^1 and 6^1 states are 1.1425 and 1.103 cm^{-1}, respectively. The observed B values of the states beyond 48 000 cm^{-1} are mostly in the range from 1.10 to 1.14 cm^{-1}. This fact indicates that these states possess some ν_4' and/or ν_6' mode character.

According to the ab initio calculation of the potential energy surface of electronically excited acetylene,[35,37,68] the trans-to-cis isomerization barrier exists around 47 000 cm^{-1}, which is close to the 3^6 state. In more detail, there are three barriers: one is in-plane (but not through the linear symmetric geometry, C_s), the other is torsional (C_2), and the last is through the linear symmetric configuration ($D_{\infty h}$). The barrier height is different for each. The trans bending vibration becomes an inversion motion only through the $D_{\infty h}$ barrier, which lies at much higher energy than the lowest trans-to-cis isomerization barrier. Around any of these barriers, there is enormously strong anharmonic coupling between overtones and combinations involving the three bending modes (ν_3', ν_4', and ν_6'), and the level structure becomes much more complicated. The analysis of our identified vibrational-level structure in terms of the vibrational modes including the inversion motion is our future task since more detailed information is needed on the vibrational dynamics in the $\tilde{A}$ state far below the barrier. Work in line with this objective has just started in our group.[53]

In the energy region above the adiabatic dissociation threshold of 49 767 cm^{-1}, the LIF intensities become extremely weak, but still the observed bands are composed of a rotational structure that is essentially similar to that of the 3^n ($n \leq 5$) or 2^13^n ($n \leq 4$) state as shown in Figure 3b. This implies that the excited acetylene at the highest energy in our experiment still predissociates and that the Franck−Condon-allowed vibrational state couples only weakly with the motion along the dissociation coordinate toward $C_2H + H$.

H-Atom Action Spectrum. In Figure 2b, the observed H-atom action spectrum is compared with the LIF spectrum. It

is obvious that the H-atom action spectrum is composed of the spectral lines common to those of the LIF spectrum though the line intensities are different in the two spectra. In the higher-energy region, the LIF line intensities are reduced, but the reverse is the case for the H-atom action spectrum. This implies that the lifetimes of the excited states tend to be shorter at the higher energies because of more efficient electronic relaxation including the dissociation reaction. According to Suzuki and Hashimoto's measurement of the fluorescence quantum yield,[20] its magnitude of the 3^5K^1 state is on the order of 10^{-4}. This value is consistent with the lifetime of 100 ps determined from the observed line width (discussed later) since the fluorescence lifetime of the pure singlet state is around 300 ns.[21,22] The shortening of the lifetime would be caused by an increased predissociation rate constant of acetylene excited in a higher-energy region. However, the quantum yield for the production of H atoms in the photodissociation at 193.3 nm was reported to be 0.26[69] and 0.3.[70] This indicates that a large fraction of excited acetylene relaxes to metastable states, possibly including isomerization to vinylidene.

In the excitation-energy region beyond 48 000 cm^{-1}, the number of observed bands increases, and the H-atom action spectral lines become more intense. As already pointed out, the increase of the excited-level density is attributable to the anharmonic resonance between the Franck−Condon-allowed gerade ν_2' and ν_3' modes and the forbidden ungerade ν_4' and ν_6' modes. According to Cui and Morokuma's ab initio calculation[37] of the potential energy surfaces, the triplet state-mediated photodissociation starts over the minima on the seam of crossing between the S_1 and T_3 states in C_2 symmetry. Thus, the gerade H−C−C bending ν_3' mode as well as the ungerade ν_4' and ν_6' modes could be promoting vibrational motions for the conversion from S_1 acetylene in C_{2h} symmetry to T_3 and furthermore to T_2 with the torsion angle of around 100° and finally to T_1 through which the dissociation reaction proceeds. Thus, if the 3^n states couple with the 4^i6^j states ($i + j =$ even) through anharmonic resonance, the resultant states could be more likely to predissociate. This statement seems to contradict our recent finding on the S−T coupling in the ungerade vibrational states, 3^36^1 and 3^34^1, of which only the former state indicates triplet character (i.e., the ν_4' mode suppresses the S−T coupling). However, we speculate that the dissociation reaction proceeds via the conversion of the stationary states to nonstationary dissociative states through triplet states. In the stationary state, the S−T coupling is possible only in C_{2h} geometry, whereas this stationary state couples to the continuum dissociative state through triplet states as intermediates. Referring to the calculated surface,[37] the ν_3' bending and ν_4' torsion may contribute to the motion along the seam of the S_1 and T_3 crossing from C_{2h} geometry to C_2 toward the energy minimum.

The threshold energy for the adiabatic dissociation of acetylene in the Ã state is supposed to be 49 767 cm^{-1} if the energy difference between the Ã and $\tilde{X}$ states of C_2H is assumed to be 3693 cm^{-1}.[13,14] In the region beyond this threshold energy, several intense bands (48−53) appear in the H-atom action spectrum, indicating efficient photodissociation. However, the direct dissociation would not occur on the dissociative surface of the Ã state since the bands consist of the rotational transition lines with widths of around 0.1 cm^{-1}(discussed later), which implies that the dissociation proceeds through a long-lived excited state.

Lifetime of Excited Acetylene. In the excitation-energy region of the present experiment (47 000−50 600 cm^{-1}), excited acetylene predissociates with a lifetime much longer than the rotational period. To evaluate the lifetime of acetylene in respective rovibrational states from the line width, some of the LIF spectral lines were observed at high resolution by inserting an etalon into the dye laser cavity. The observed line widths are corrected by subtracting the excitation laser-line width and are converted to decay rates (i.e., the reciprocal lifetimes), which are plotted in Figure 5 as a function of the excitation energy. It is seen that the decay rate constant of the rovibronic state increases almost in proportion to the excitation energy up to around 4×10^{10} s^{-1} at the highest energy of 50 600 cm^{-1}, which exceeds the adiabatic dissociation threshold in the Ã state by 933 cm^{-1}. If the reaction mechanism changes at a certain energy region from the triplet state-mediated photodissociation to the direct dissociation on the Ã state potential energy surface, then the lifetime of excited acetylene should reflect this situation. However, because of the wavelength limitation of the third harmonic of the dye laser, we could not reach an energy region where the dissociation mechanism changes.

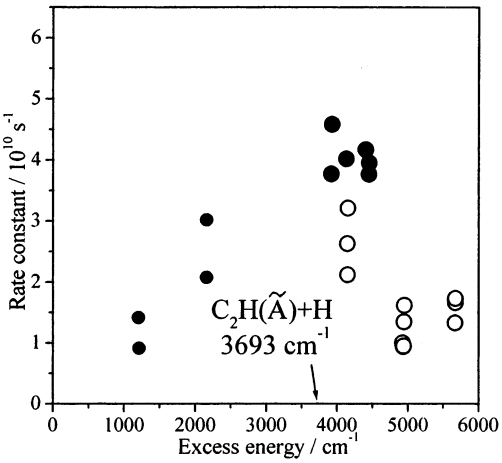

Figure 5. Excess energy dependence of the decay rate constants determined from the observed LIF line widths. The excess energy is defined as the excitation energy minus the dissociation threshold energy, 46 074 cm^{-1}. Data of the gerade (●) and ungerade (○) vibrational states are shown. Two data points at an excess energy around 2000 cm^{-1} are those calculated from the LIF line width data in ref 66. The Ã state of C_2H located at 3693 cm^{-1} [13,14] is also shown.

To observe the line widths of the transitions in the region beyond the 193.3 nm photon energy, acetylene in the vibrational excited ν_3'' state in the $\tilde{X}$ state, which was prepared by irradiation with an IR laser, was excited further by the UV laser. By utilizing this IR−UV double-resonance method, the highest excitation energy given to acetylene can be 53 500 cm^{-1}, which corresponds to 187 nm. In Figure 6a−d, our observed IR−UV double-resonance spectra are shown in which acetylene was excited first to the $J'' = 0$ or 2 level of the ν_3'' vibrational state and then excited further to allowed rotational levels of the ungerade vibrational state. The allowed rotational transition from $J'' = 0$ is only the R-branch transition to $J' = 1$, whereas from $J'' = 2$, P, Q, and R transitions are possible to $J' = 1$, 2, and 3, respectively. The line width in the lower-energy region, 50 220−50 230 cm^{-1} (d), is larger than those in the higher-energy region of 51 010−51 025 cm^{-1} (c) or 51 745−51 755 cm^{-1} (a, b). The line widths are converted to the decay rates of respective excited states, which are plotted in Figure 5 as open circles as a function of the excess energy. It is seen that beyond the excess energy of 4500 cm^{-1} for the production of $C_2H(\tilde{X}) + H$, which corresponds to the excitation energy of 51 100 cm^{-1}, the decay rate is reduced significantly to around 1×10^{10} s^{-1}, which is $^1/_4$ of the maximum value at an excess energy of 4000 cm^{-1}. This is opposite to the expectation that the activated molecules

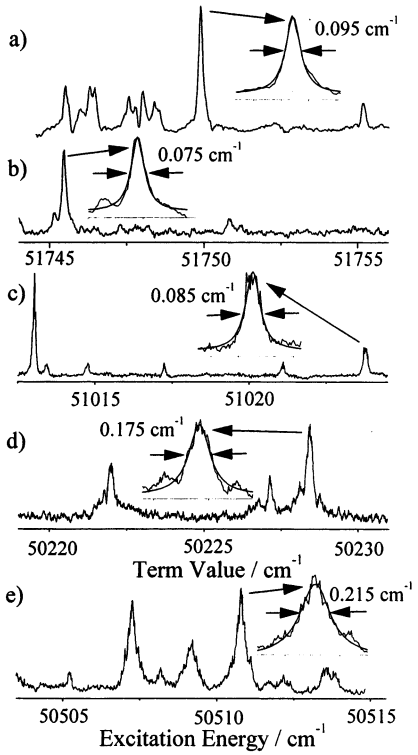

Figure 6. (a)−(d) IR−UV double-resonance spectra of the transitions to the ungerade states and (e) one-photon spectra of the transitions to the gerade state in a similar energy region to that of spectrum d. One of the peaks in each spectrum is magnified to show the line shape and line width. The values of the line widths show the corrected values that are the observed line widths minus the laser line widths. In the IR−UV double-resonance spectra, the energy on the abscissa is the term value, which is defined as the rovibrational energy of the $\tilde{X}$ state plus the UV photon energy.

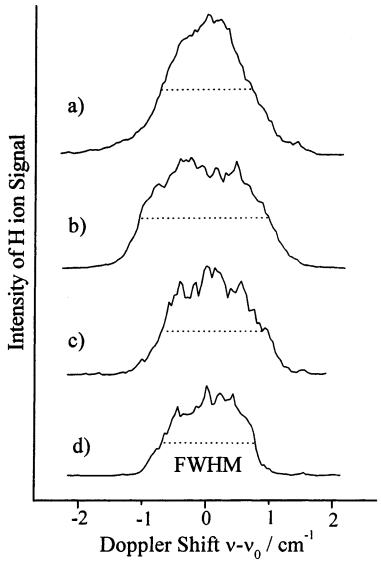

Figure 7. Doppler line profile of the REMPI spectral line of the produced H atoms observed with different excess energies, which are defined as the excitation energy minus the dissociation threshold energy of 46 074 cm^{-1}: (a) 6654 cm^{-1}, (b) 4422 cm^{-1}, (c) 3514 cm^{-1}, (d) 1192 cm^{-1}.

with higher energies tend to surmount the transition state with larger rates. A possible interpretation of this fact is that the dissociation mechanism changes from the triplet state-mediated dissociation to the direct dissociation on the $\tilde{A}$ state potential energy surface in the excitation energy region around 51 100 cm^{-1}. However, it remains unsolved why the triplet state-mediated dissociation ceases suddenly. Further theoretical or experimental work is desired for a clarification of the present finding of the sudden change of the dissociation rate.

In the nascent state distribution of C_2H in the 193.3 nm photodissociation observed by Hsu et al.,[44] the bending vibration is extensively excited, and this was attributed to a dissociation mechanism through a narrow transition state that may be located at the barrier on the $\tilde{A}$ state potential energy surface toward the product C_2H ($\tilde{A}$ or $\tilde{X}$) + H. They also suggest a change in the photodissociation mechanism from a triplet state-mediated dissociation to a direct dissociation on the $\tilde{A}$ state potential energy surface at an energy higher than 6.1 eV (49 000 cm^{-1}). Their proposal is essentially in accord with the present finding.

Since the electronic transition is to the $\tilde{A}^1A_u$ state from the $\tilde{X}^1\Sigma_g^+$, the upper vibrational state must have the same parity as that of the lower state; in the present experiment of the IR−UV double-resonance excitation, the ν_3'' state of the $\tilde{X}$ state is ungerade as to the inversion symmetry operation so that the upper vibrational state of the $\tilde{A}$ state must be also ungerade. An important question to be discussed here is whether the photodissociation mechanism or efficiency of acetylene in the gerade vibrational state differs from that of the ungerade state. Referring to Figure 5, it is seen that the observed decay constants of the ungerade rovibrational levels are on the same order of magnitude as those of the gerade levels just beyond the adiabatic dissociation threshold of the $\tilde{A}$ state, though most of the decay constants are a little smaller than those of the gerade rovibrational levels in the similar excitation-energy region. In an earlier section, we pointed out that the anharmonic resonance between the ν_3' and ν_4'/ν_6' vibrational modes results in a polyad vibrational level structure. This statement can also be applied to the ungerade vibrational states in the $\tilde{A}$ state. The difference between the gerade and ungerade vibrational states is simply due to whether the state involves the contribution of the vibrational state with the even or odd quantum number of the ν_4'/ν_6' vibrational mode. If the anharmonic couplings among the ν_3' and ν_4'/ν_6' vibrational modes are significant, then the dissociation efficiencies of the gerade and ungerade excited states must be essentially equal in the same excitation energies.

Kinetic Energy of the H Atom. Figure 7 shows the observed REMPI spectral lines of H atoms produced by the photodissociation of acetylene excited to various levels of the excess energies from 1193 to 6654 cm^{-1}. The line shapes are of a trapezoidal form, indicating that the lifetime of the excited acetylene is long enough to result in the isotropic scattering of fragments C_2H and H. This observation is essentially similar to that by Suzuki and co-workers.[17,18] Mordaunt et al.[12] found anisotropic scattering of C_2H in a low rotational level in the predissociation of acetylene in the $2^13^5K^1$ state. However, in the corresponding energy region of our Doppler width measurements, the line shape can still be interpreted as that of the isotropically scattered H atoms, though they are detected parallel to the laser polarization. This could be attributed to the fact that the anisotropically scattered H atoms contribute to the line shape to a lesser extent than do the isotropically scattered atoms. In the higher excitation-energy region beyond 50 000 cm^{-1}, the line shape becomes closer to a triangle form. This is probably caused by a wide distribution of the kinetic energy of the produced H atoms. According to Balko et al.'s TOF measurements[10] of the H atoms produced from the 193.3 nm photodissociation of acetylene, the translation energy distributes up to 15 kcal mol^{-1} with an average energy of about 6 kcal mol^{-1}

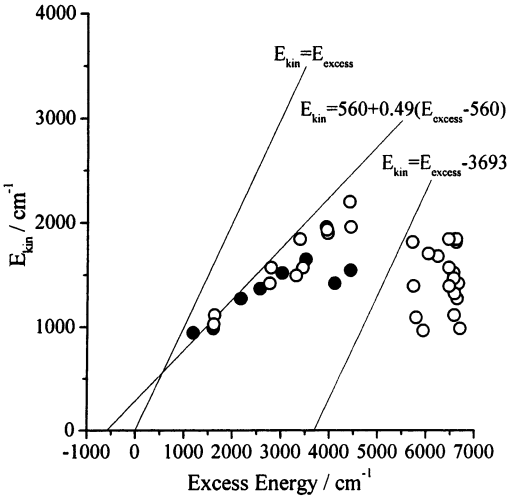

Figure 8. Excess energy dependence of the average kinetic energy of the H atom evaluated from the Doppler line profile. The excess energy is defined as the excitation energy minus the dissociation threshold energy of 46 074 cm^{-1}. Data from the gerade (●) and ungerade (○) vibrational states.

(2100 cm^{-1}), which is close to our determined average kinetic energy of H atoms given in Figure 8.

Suzuki and co-workers[17,18] proposed the relationship between the excess energy and the kinetic energy of H atoms: $E_{kin}/cm^{-1} = 560 + 0.49\ (E_{excess} - 560)$, where the first term represents the height of the exit barrier for dissociation. This relationship is almost in agreement with our data on the excitation energies of $E_{excess} \lesssim 4000\ cm^{-1}$. Beyond this energy, the average kinetic energy is reduced a little and takes scattered values between 1000 and 2000 cm^{-1}. This fact must be closely related to the observation described in the former section that the decay rate takes a maximum value around $E_{excess} \approx 4000\ cm^{-1}$ and is reduced to a value about $^1/_4$ of the maximum value above this energy. Thus, the present finding on the kinetic energy also supports the previous conclusion that the photodissociation proceeds on the $\tilde{A}$ state surface beyond the excitation energy of 50 600 cm^{-1} ($E_{excess} \approx 4500\ cm^{-1}$). According to Hsu et al.'s state analysis[44] of the fragment C_2H produced in the 193.3 nm photodissociation, a large fraction of C_2H is highly excited in the bending mode in the $\tilde{X}$ state. However, these C_2H molecules carry a large fraction of $\tilde{A}$ state character because of strong vibronic coupling between the $\tilde{X}$ and $\tilde{A}$ states.

Our observed values of E_{kin} are independent of the vibrational parity of the initial excited state. In Figure 8, the filled circles are the data obtained from acetylene excited to the gerade vibrational state by one photon of UV excitation, whereas the open circles are those from acetylene excited to the ungerade vibrational state by the IR−UV double-resonance method. Both sets of data are in agreement within a factor of less than 2. This may be further evidence that the ν_3' and ν_4'/ν_6' vibrational modes couple with each other because of anharmonic resonance in this energy region.

Conclusions

(1) In the $\tilde{A}$ state of acetylene, 60 gerade vibrational states could be identified in the energy range of 47 000−50 600 cm^{-1}, most of which are originated from anharmonic couplings between the Franck−Condon-allowed 2^m3^n states and the 4^i6^j ($i + j$ = even) vibrational states.

(2) Excited acetylene predissociates with a lifetime of 100 ps at an excitation energy of 47 000 cm^{-1}, which is shortened at higher excitation energy up to 25 ps at 50 600 cm^{-1}. Beyond it, the lifetime lengthens to around 100 ps. This change in the lifetime is attributed to the dissociation mechanism changing from the triplet state-mediated dissociation to the direct dissociation on the potential energy surface of the $\tilde{A}$ state.

(3) For the excitation energies up to the adiabatic dissociation threshold of the $\tilde{A}$ state, the average kinetic energy, E_{kin}, of the produced H atoms is almost in agreement with $E_{kin}/cm^{-1} = 560 + 0.49(E_{excess} - 560)$. Beyond the threshold, the kinetic energies are around 1000−2000 cm^{-1}, which is a little smaller than the excess energy for the production of $C_2H(\tilde{A}) + H$. This fact indicates that the dissociation proceeds on the $\tilde{A}$ state surface in this energy region.

(4) Evidence could not be found to indicate that the predissociation mechanism or efficiency is dependent on the vibrational parity, gerade or ungerade, of excited acetylene in the $\tilde{A}$ state.

Acknowledgment. N.Y. and S.T. acknowledge partial support for the present work by a Grant-in-Aid from the Ministry of Education, Science, Culture and Sports (contract no. 13640518). We thank Professor R. W. Field for his valuable comments and Professor H. Kanamori for his computational help on the rotational analysis.

References and Notes

(1) Wodtke, A. M.; Lee, Y. T. *J. Phys. Chem.* **1985**, *89*, 4744.
(2) Shiromaru, H.; Achiba, Y.; Kimura, K.; Lee, Y. T. *J. Phys. Chem.* **1987**, *91*, 17.
(3) Chen, Y.; Jonas, D.; Hamilton, C.; Green, P. G.; Kinsey, J. L.; Field, R. W. *Ber. Bunsen-Ges. Phys. Chem.* **1988**, *92*, 329.
(4) Fujii, M.; Tanabe, S.; Okuzawa, Y.; Ito, M. *Laser Chem.* **1994**, *14*, 161.
(5) Segall, J.; Lavi, R.; Wen, Y.; Wittig, C. *J. Phys. Chem.* **1989**, *93*, 7287.
(6) Green, P. G.; Kinsey, J. L.; Field, R. W. *J. Chem. Phys.* **1989**, *91*, 5160.
(7) Baldwin, D. P.; Buntine, M. A.; Chandler, D. W. *J. Chem. Phys.* **1990**, *93*, 6578.
(8) Ervin, K. M.; Gronert, S.; Barlow, S. E.; Gilles, M. K.; Harrison, A. G.; Bierbaum, V. M.; DePuy, C. H.; Lineberger, W. C.; Ellison, G. B. *J. Am. Chem. Soc.* **1990**, *112*, 5750.
(9) Ruscic, B.; Berkowitz, J. *J. Chem. Phys.* **1990**, *93*, 5586.
(10) Balko, B. A.; Zhang, J.; Lee, Y. T. *J. Chem. Phys.* **1991**, *94*, 7958.
(11) Segall, J.; Wen, Y.; Lavi, R.; Singer, R.; Wittig, C. *J. Phys. Chem.* **1991**, *95*, 8078.
(12) Mordaunt, D. H.; Ashfold, M. N. R. *J. Chem. Phys.* **1994**, *101*, 2630.
(13) Carrick, P. G.; Merer, A. J.; Curl, R. F. *J. Chem. Phys.* **1983**, *78*, 3652.
(14) Curl, R. F.; Carrick, P. G.; Merer, A. J. *J. Chem. Phys.* **1985**, *82*, 3479.
(15) Fujii, M.; Haijima, A.; Ito, M. *Chem. Phys. Lett.* **1988**, *150*, 380.
(16) Haijima, A.; Fujii, M.; Ito, M. *J. Chem. Phys.* **1990**, *92*, 959.
(17) Hashimoto, N.; Suzuki, T. *J. Chem. Phys.* **1996**, *104*, 6070.
(18) Hashimoto, N.; Yonekura, N.; Suzuki, T. *Chem. Phys. Lett.* **1997**, *264*, 545.
(19) Mordaunt, D. H.; Ashfold, M. N. R.; Dixon, R. N.; Loffler, P.; Schnieder, L.; Welge, K. H. *J. Chem. Phys.* **1998**, *108*, 519.
(20) Suzuki, T.; Hashimoto, N. *J. Chem. Phys.* **1999**, *110*, 2042.
(21) Ochi, N.; Tsuchiya, S. *Chem. Phys. Lett.* **1987**, *140*, 20.
(22) Ochi, N.; Tsuchiya, S. *Chem. Phys.* **1991**, *152*, 319.
(23) Yamakita, N.; Tsuchiya, S. *Chem. Phys. Lett.* **2001**, *348*, 53.
(24) Dupre, P.; Green, P. G.; Field, R. W. *Chem. Phys.* **1995**, *196*, 211.
(25) Dupre, P. D.; Jost, R.; Lombardi, M.; Green, P. G.; Abramson, E.; Field, R. W. *Chem. Phys.* **1991**, *152*, 293.
(26) Dupre, P. *Chem. Phys.* **1995**, *196*, 239.
(27) Suzuki, T.; Shi, Y.; Kohguchi, H. *J. Chem. Phys.* **1997**, *106*, 5292.
(28) Shi, Y.; Suzuki, T. *J. Phys. Chem. A* **1998**, *102*, 7414.
(29) Humphrey, S. J.; Morgan, C. G.; Wodtke, A. M.; Cunningham, K. L.; Drucker, S.; Field, R. W. *J. Chem. Phys.* **1997**, *107*, 49.
(30) Altunata, S.; Field, R. W. *J. Chem. Phys.* **2000**, *113*, 6640.
(31) Peric, M.; Buenker, R. J.; Peyerimhoff, S. D. *Mol. Phys.* **1984**, *53*, 1177.
(32) Peric, M.; Peyerimhoff, S. D.; Buenker, R. J. *Mol. Phys.* **1985**, *55*, 1129.

(33) Peric, M.; Peyerimhoff, S. D.; Buenker, R. J. *Mol. Phys*. **1987**, *62*, 1339.
(34) Lischka, H.; Karpfen, A. *Chem. Phys*. **1986**, *102*, 77.
(35) Osamura, Y.; Mitsuhashi, F.; Iwata, S. *Chem. Phys. Lett*. **1989**, *164*, 205.
(36) Cui, Q.; Morokuma, K.; Stanton, J. F. *Chem. Phys. Lett*. **1996**, *263*, 46.
(37) Cui, Q.; Morokuma, K. *Chem. Phys. Lett*. **1997**, *272*, 319.
(38) Zhang, J.; Riehn, C. W.; Dulligan, M.; Wittig, C. *J. Chem. Phys*. **1995**, *103*, 6815.
(39) Arusi-Parpar, T.; Schmid, R. P.; Li, R.-J.; Bar, I.; Rosenwaks, S. *Chem. Phys. Lett*. **1997**, *268*, 163.
(40) Schmid, R. P.; Arusi-Parpar, T.; Li, R.-J.; Bar, I.; Rosenwaks, S. *J. Chem. Phys*. **1997**, *107*, 385.
(41) Arusi-Parpar, T.; Schmid, R. P.; Ganot, Y.; Bar, I.; Rosenwaks, S. *Chem. Phys. Lett*. **1998**, *287*, 347.
(42) Schmid, R. P.; Ganot, Y.; Bar, I.; Rosenwaks, S. *J. Chem. Phys*. **1998**, *109*, 8959.
(43) Fletcher, T. R.; Leone, S. R. *J. Chem. Phys*. **1989**, *90*, 871.
(44) Hsu, Y.-C.; Chen, F.-T.; Chou, L.-C.; Shiu, Y.-J. *J. Chem. Phys*. **1996**, *105*, 9153.
(45) Van Craen, J. C.; Herman, M.; Colin, R.; Watson, J. K. G. *J. Mol. Spectrosc*. **1986**, *119*, 137.
(46) Utz, A. L.; Tobiason, J. D.; Carrasquillo, M. E.; Sanders, J. L.; Crim, F. F. *J. Chem. Phys.* **1993**, *98*, 2742.
(47) Tobiason, J. D.; Utz, A. L.; Crim, F. F. *J. Chem. Phys*. **1993**, *99*, 928.
(48) Tobiason, J. L.; Utz, A. L.; Sibert, E. L., III; Crim, F. F. *J. Chem. Phys*. **1993**, *99*, 5762.
(49) Mizoguchi, M.; Yamakita, N.; Tsuchiya, S.; Iwasaki, A.; Hoshina, K.; Yamanouchi, K. *J. Phys. Chem*. *A* **2000**, *104*, 10212.
(50) Auwera, J. V.; Hurtmans, D.; Carleer, M.; Herman, M. *J. Mol. Spectrosc*. **1993**, *157*, 337.
(51) Watson, J. K. G.; Herman, M.; Van Craen, J. C.; Colin, R. *J. Mol. Spectrosc*. **1982**, *95*, 101.
(52) Van Craen, J. C.; Herman, M.; Colin, R.; Watson, J. K. G. *J. Mol. Spectrosc*. **1985**, *111*, 185.
(53) Merer, A. J.; Yamakita, N.; Tsuchiya, S.; Stanton, J. F.; Duan, Z.; Field, R. W. *Mol. Phys.*, in press.
(54) Scherer, G. J.; Chen, Y.; Redington, R. L.; Kinsey, J. L.; Field, R. W. *J. Chem. Phys*. **1986**, *85*, 6315.
(55) Drabbels, M.; Heinze, J.; Meerts, W. L. *J. Chem. Phys*. **1994**, *100*, 165.
(56) Yamanouchi, K.; Ikeda, N.; Tsuchiya, S.; Jonas, D. M.; Lundberg, J. K.; Adamson, G. W.; Field, R. W. *J. Chem. Phys*. **1991**, *95*, 6330.
(57) Abbouti Temsamani, M.; Herman, M.; Solina, S. A. B.; O'Brien, J. P.; Field, R. W. *J. Chem. Phys*. **1996**, *105*, 11357.
(58) Solina, S. A. B.; O'Brien, J. P.; Field, R. W.; Polik, W. F. *Ber. Bunsen-Ges. Phys. Chem*. **1995**, *99*, 555.
(59) Solina, S. A. B.; O'Brien, J. P.; Field, R. W.; Polik, W. F. *J. Phys. Chem*. **1996**, *100*, 7797.
(60) O'Brien, J. P.; Jacobson, M. P.; Sokol, J. J.; Coy, S. L.; Field, R. W. *J. Chem. Phys*. **1998**, *108*, 7100.
(61) Jacobson, M. P.; O'Brien, J. P.; Silbey, R. J.; Field, R. W. *J. Chem. Phys*. **1998**, *109*, 121.
(62) Jacobson, M. P.; O'Brien, J. P.; Field, R. W. *J. Chem. Phys*. **1998**, *109*, 3831.
(63) Jonas, D. M.; Solina, S. A. B.; Rajaram, B.; Silbey, R. J.; Field, R. W.; Yamanouchi, K.; Tsuchiya, S. *J. Chem. Phys*. **1992**, *97*, 2813.
(64) Jonas, D. M.; Solina, S. A. B.; Rajaram, B.; Silbey, R. J.; Field, R. W.; Yamanouchi, K.; Tsuchiya, S. *J. Chem. Phys*. **1993**, *99*, 7350.
(65) Hoshina, K.; Iwasaki, A.; Yamanouchi, K.; Jacobson, M. P.; Field, R. W. *J. Chem. Phys*. **2001**, *114*, 7424.
(66) Kellman, M. E.; Chen, G. *J. Chem. Phys*. **1991**, *95*, 8671.
(67) Tsuji, K.; Terauchi, C.; Shibuya, K.; Tsuchiya, S. *Chem. Phys. Lett*. **1999**, *306*, 41.
(68) Stanton, J. F.; Huang, C.-M.; Szalay, P. G. *J. Chem. Phys*. **1994**, *101*, 356.
(69) Satyapal, S.; Bersohn, R. *J. Phys. Chem*. **1991**, *95*, 8004.
(70) Seki, K.; Okabe, H. *J. Phys. Chem*. **1993**, *97*, 5284.